

Temperature Dependence of the Rate Constants and Branching Ratios for the Reactions of $\text{Cl}^-(\text{D}_2\text{O})_{1-3}$ with CH_3Br and Thermal Dissociation Rates for $\text{Cl}^-(\text{CH}_3\text{Br})$

John V. Seeley,^{†,‡} Robert A. Morris,[‡] A. A. Viggiano,^{*,‡} Haobin Wang,[§] and William L. Hase[§]

Contribution from Phillips Laboratory, Geophysics Directorate, Ionospheric Effects Division (GPID), 29 Randolph Road, Hanscom AFB, Massachusetts 01731-3010, and Department of Chemistry, Wayne State University, Detroit, Michigan 48202

Received March 18, 1996[Ⓢ]

Abstract: The rate constants and products for the reactions of $\text{Cl}^-(\text{D}_2\text{O})_n + \text{CH}_3\text{Br}$ ($n = 1-3$) have been measured. The $n = 1$ reaction was studied from 238 to 478 K. The rate constant is well described by $k = (6.0 \times 10^{-10}) \exp(-1270/T) \text{ cm}^3 \text{ s}^{-1}$. We determined the reaction mechanism to be ligand switching to produce $\text{Cl}^-(\text{CH}_3\text{Br})$ followed by thermal decomposition of the complex. $\text{Cl}^-(\text{CH}_3\text{Br})$ decomposition produces greater than 90% $\text{Br}^- + \text{CH}_3\text{Cl}$ with the remainder being $\text{Cl}^- + \text{CH}_3\text{Br}$. The $\text{Cl}^-(\text{CH}_3\text{Br}) + \text{He}$ rate constant is well described by $k = (4.5 \times 10^{-10}) \exp(-2260/T) \text{ cm}^3 \text{ s}^{-1}$. RRKM theory was used to model the decomposition of $\text{Cl}^-(\text{CH}_3\text{Br})$. The results are consistent with our experimental results if a central barrier height of 22.5 kJ mol^{-1} is used. The $n = 2$ and 3 reactions also proceed by ligand switching followed by thermal decomposition. The $n = 2$ reaction was studied from 203 to 298 K. The rate constant is well-described by $(4.4 \times 10^{-9}) \exp(-1329/T) \text{ cm}^3 \text{ s}^{-1}$. The main product observed was $\text{Cl}^-(\text{D}_2\text{O})$ with a smaller amount of $\text{Cl}^-(\text{D}_2\text{O})(\text{CH}_3\text{Br})$ also detected. The $n = 3$ reaction was studied from 188 to 203 K. The reaction was about a factor of 1.8 faster than the $n = 2$ reaction. The main product was $\text{Cl}^-(\text{D}_2\text{O})_2$ with smaller amounts of $\text{Cl}^-(\text{D}_2\text{O})_2(\text{CH}_3\text{Br})$ and $\text{Cl}^-(\text{D}_2\text{O})(\text{CH}_3\text{Br})$ also observed.

Introduction

The gas-phase $\text{S}_{\text{N}}2$ reaction of $\text{Cl}^- + \text{CH}_3\text{Br}$ has been well studied experimentally and theoretically.¹⁻¹⁵ This reaction is believed to proceed along a double-well potential energy surface with a central barrier that separates the entrance and exit channel complexes. Although statistical theories, such as RRKM theory, have been used to model $\text{S}_{\text{N}}2$ reactions,⁸ the $\text{Cl}^- + \text{CH}_3\text{Br}$ reaction has been shown^{2-4,13-18} to be inadequately described by such theories.

The goal of this work was to study the effects of hydration of Cl^- on its reaction with CH_3Br . Interest in solvation

effects involving $\text{S}_{\text{N}}2$ reactions has a long history.¹⁹⁻²⁵ In general, solvation is thought to stabilize the reactants more than it does the transition state located at the central barrier.¹⁹ As a result, the relative barrier height increases and the fraction of reaction adducts which dissociate to regenerate the reactants increases at the expense of those that are transformed into products. Thus, rate constants are often observed to decrease substantially with increasing solvation. Previous solvation studies on the $\text{Cl}^- + \text{CH}_3\text{Br}$ reaction have focused on solvents other than water. Bohme and Raksit²¹ and Giles and Grimsrud²⁶ both found that the addition of a variety of organic solvent molecules to Cl^- greatly reduced the reaction rate.

We find that hydration also slows down the $\text{S}_{\text{N}}2$ channel. However, instead of the reaction stopping upon solvation, the reaction mechanism changes to ligand switching. In addition, we find that the $\text{Cl}^-(\text{CH}_3\text{Br})$ product of the $\text{Cl}^-(\text{D}_2\text{O}) + \text{CH}_3\text{Br}$ reaction can be observed in our flow tube, allowing the thermal breakup rate of $\text{Cl}^-(\text{CH}_3\text{Br})$ to be determined as a function of temperature. We have performed RRKM calculations to complement our experimental results.

* Author to whom correspondence should be addressed.

† Air Force Geophysics Scholar.

‡ Phillips Laboratory.

§ Wayne State University.

Ⓢ Abstract published in *Advance ACS Abstracts*, January 1, 1997.

(1) Viggiano, A. A.; Paschkewitz, J. S.; Morris, R. A.; Paulson, J. F.; Gonzalez-Lafont, A.; Truhlar, D. G. *J. Am. Chem. Soc.* **1991**, *113*, 9404.

(2) Viggiano, A. A.; Morris, R. A.; Paschkewitz, J. S.; Paulson, J. F. *J. Am. Chem. Soc.* **1992**, *114*, 10477.

(3) Graul, S. T.; Bowers, M. T. *J. Am. Chem. Soc.* **1991**, *113*, 9696.

(4) Knighton, W. B.; Bogner, J. A.; O'Conner, P. M.; Grimsrud, E. P. *J. Am. Chem. Soc.* **1993**, *115*, 12079.

(5) Cyr, D. M.; Posey, L. A.; Bishea, G. A.; Han, C.-C.; Johnson, M. A. *J. Am. Chem. Soc.* **1991**, *113*, 9697.

(6) DePuy, C. H.; Gronert, S.; Mullin, A.; Bierbaum, V. M. *J. Am. Chem. Soc.* **1990**, *112*, 8650.

(7) Gronert, S.; DePuy, C.; Bierbaum, V. *J. Am. Chem. Soc.* **1991**, *113*, 4009–4010.

(8) Olmstead, W. N.; Brauman, J. I. *J. Am. Chem. Soc.* **1977**, *99*, 4219.

(9) Tanaka, K.; Mackay, G. I.; Payzant, J. D.; Bohme, D. K. *Can. J. Chem.* **1976**, *54*, 1643–1659.

(10) Caldwell, G.; Magnera, T. F.; Kebarle, P. *J. Am. Chem. Soc.* **1984**, *106*, 959–966.

(11) Ingemann, S.; Nibbering, N. M. M. *Can. J. Chem.* **1984**, *62*, 2273–2281.

(12) Wang, H.; Zhu, L.; Hase, W. L. *J. Phys. Chem.* **1994**, *98*, 1608.

(13) Wang, W. L.; Peslherbe, G. H.; Hase, W. L. *J. Am. Chem. Soc.* **1994**, *116*, 9644.

(14) Wang, H.; Hase, W. L. *J. Am. Chem. Soc.* **1995**, *117*, 9347.

(15) Graul, S. T.; Bowers, M. T. *J. Am. Chem. Soc.* **1994**, *110*, 3875.

(16) Morris, R. A.; Viggiano, A. A. *J. Phys. Chem.* **1994**, *98*, 3740.

(17) Viggiano, A. A.; Morris, R. A.; Su, T.; Wladkowski, B. D.; Craig, S. L.; Zhong, M.; Brauman, J. I. *J. Am. Chem. Soc.* **1994**, *116*, 2213.

(18) Peslherbe, G. H.; Wang, H.; Hase, W. L. *J. Am. Chem. Soc.* In press.

(19) Bohme, D. K.; Mackay, G. I. *J. Am. Chem. Soc.* **1981**, *103*, 978.

(20) Bohme, D. K.; Raksit, A. B. *J. Am. Chem. Soc.* **1984**, *106*, 3447.

(21) Bohme, D. K.; Raksit, A. B. *Can. J. Chem.* **1985**, *63*, 3007.

(22) Henschman, M.; Hierl, P. M.; Paulson, J. F. *Adv. Chem. Ser.* **1987**, *215*, 83.

(23) Hierl, P. M.; Ahrens, A. F.; Henschman, M.; Viggiano, A. A.; Paulson, J. F.; Clary, D. C. *J. Am. Chem. Soc.* **1986**, *108*, 3142.

(24) Hierl, P. M.; Paulson, J. F.; Henschman, M. *J. Phys. Chem.* In press.

(25) Viggiano, A. A.; Arnold, S. T.; Morris, R. A.; Ahrens, A. F.; Hierl, P. M. *J. Am. Chem. Soc.* **1996**, *100*, 14397.

(26) Giles, K.; Grimsrud, E. P. *J. Phys. Chem.* **1993**, *97*, 1318.

Experimental Section

The experiments were performed in a variable-temperature selected ion flow tube (VT-SIFT). The apparatus has been described in detail elsewhere,²⁷ and only information pertinent to the present experiments will be discussed. $\text{Cl}^-(\text{H}_2\text{O})_n$ or $\text{Cl}^-(\text{D}_2\text{O})_n$ ions were produced using a supersonic expansion ion source. Ions were formed by expanding a mixture of Ar and H_2O or D_2O , held at about 4 atm of total pressure, through a 25- μm orifice and then ionizing the gas just downstream of the expansion with an electron filament (ThO_2/Ir). CF_2Cl_2 was added immediately downstream of the expansion. The CF_2Cl_2 was entrained in the expansion to produce $\text{Cl}^-(\text{H}_2\text{O})_n$ ions in a manner similar to that used by Johnson and colleagues.²⁸ The ions were sampled by a blunt skimmer and passed into a quadrupole mass filter.

To study the reactions of $\text{Cl}^-(\text{D}_2\text{O})$ or $\text{Cl}^-(\text{H}_2\text{O})$, we injected that particular cluster ion into the flow tube and obtained signals of ~50–90% purity, the remainder being Cl^- due to dissociation. Less dissociation was seen at lower temperatures. To study $\text{Cl}^-(\text{D}_2\text{O})_n$ with $n \geq 2$, we used three techniques, all of which produced the same experimental results: (1) We injected $\text{Cl}^-(\text{D}_2\text{O})_n$ and obtained about 20% $\text{Cl}^-(\text{D}_2\text{O})_n$ and 80% $\text{Cl}^-(\text{D}_2\text{O})_{n-1}$. (2) We injected $\text{Cl}^-(\text{D}_2\text{O})_{n+1}$ at a higher injection energy chosen to dissociate one of the solvent molecules upon injection. This allowed the ion of interest to be nearly 80% of the total ion current at low temperatures, while smaller amounts were obtained at higher temperatures. (3) We injected a broad distribution of large clusters by turning the DC off in the upstream quadrupole and setting that quadrupole to allow only $\text{Cl}^-(\text{D}_2\text{O})_{n>4}$ ions to be injected. The flow tube temperature was then set so that all clusters larger than the desired cluster thermally decomposed in the upstream portion of the flow tube. At room temperature this resulted in about 15% $\text{Cl}^-(\text{D}_2\text{O})_2$ and 85% $\text{Cl}^-(\text{D}_2\text{O})$. At 233 K, this resulted in 97% $\text{Cl}^-(\text{D}_2\text{O})_2$, 2% $\text{Cl}^-(\text{D}_2\text{O})$, and <1% $\text{Cl}^-(\text{D}_2\text{O})_3$. At 200 K, the resulting distribution was 55% $\text{Cl}^-(\text{D}_2\text{O})_3$ and 45% $\text{Cl}^-(\text{D}_2\text{O})_2$ with a negligible amount of $\text{Cl}^-(\text{D}_2\text{O})$. The last technique gave the largest signals since many clusters in the primary distribution compressed into 1 or 2 main peaks. Only the reactions of the cluster with the largest value of n and reasonable signal intensity were studied using this method.

Both H_2O and D_2O were used for $n = 1$. In order to avoid the mass coincidence problem of $^{35}\text{Cl}^-(\text{H}_2\text{O})$ with $\text{OH}^-(\text{H}_2\text{O})_2$, we adjusted the upstream quadrupole to inject only $^{37}\text{Cl}^-(\text{H}_2\text{O})$. For $\text{Cl}^-(\text{H}_2\text{O})_{n>1}$, the requisite high resolution of the upstream quadrupole resulted in considerable mass discrimination and insufficient signal intensity for kinetics studies. Thus for $n > 1$, data are available only for D_2O clusters.

The reactant ions are thermalized by undergoing approximately 50 000 collisions before reaching the port where CH_3Br is injected. The CH_3Br was added without purification. At low temperatures the reactant inlet was heated to prevent freezing in the inlet line.²⁹ The CH_3Br had extremely low levels of reactive impurities. In particular, we found that the maximum HBr concentration was approximately 100 parts per million (ppm).²⁵ This is important since some of the rate constants reported here occur on only 1 in 10^3 collisions and therefore an HBr impurity substantially larger than 100 ppm would affect the results.

In order to minimize the breakup of clusters during sampling, we biased our sampling orifice at only 2.5 V and the next electrode at <25 V. Based on our analysis of the kinetics data (see the Results section), these settings allowed the $\text{Cl}^-(\text{D}_2\text{O})$ clusters to be sampled with <5% breakup. This small amount of breakup did not affect our ability to determine rate constants; however, it limited the determination of the $\text{Cl}^-(\text{CH}_3\text{Br})$ decomposition branching fractions.

Uncertainty in the absolute rate constants is estimated as 25%, and the uncertainty in the relative rate constants is 15%.³⁰ Product branching fractions were calculated without a mass discrimination correction. The

(27) Arnold, S. T.; Morris, R. A.; Viggiano, A. A. *J. Chem. Phys.* **1995**, *103*, 9242.

(28) Posey, L. A.; DeLucca, M. J.; Campagnola, P. J.; Johnson, M. A. *J. Phys. Chem.* **1989**, *93*, 1178.

(29) Viggiano, A. A.; Dale, F.; Paulson, J. F. *J. Chem. Phys.* **1988**, *88*, 2469.

(30) Viggiano, A. A.; Morris, R. A.; Dale, F.; Paulson, J. F.; Giles, K.; Smith, D.; Su, T. *J. Chem. Phys.* **1990**, *93*, 1149–1157.

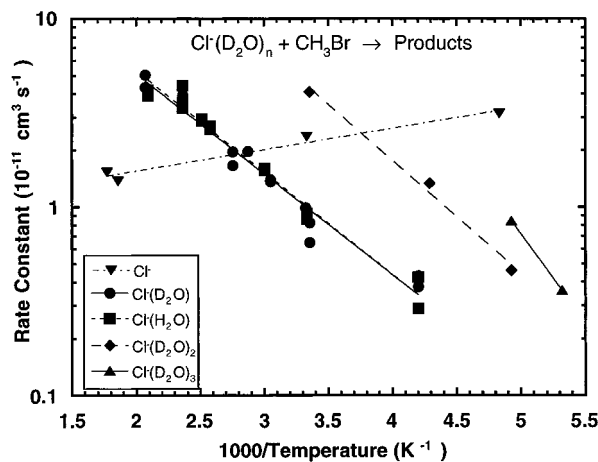


Figure 1. Arrhenius plot of the rate constants for the reactions of $\text{Cl}^-(\text{D}_2\text{O})_{0-3}$ and $\text{Cl}^-(\text{H}_2\text{O})$ with CH_3Br .

Table 1. Experimental Product Percentages for the Reaction of $\text{Cl}^-(\text{D}_2\text{O}) + \text{CH}_3\text{Br}$

temp (K)	exptl values ^a		
	% Br^-	% $(\text{BrCH}_2\text{Cl})^-$	% $(\text{BrCH}_2\text{Cl})(\text{D}_2\text{O})^-$
241	77	20	3
273	88	12	
298	94	6	
328	98	2	
363	99	1	

^a Does not include the Cl^- channel.

correction is minimized by taking data under low-resolution conditions, and the branching fractions are expected to be accurate to within 5–10 percentage units.

Results

Figure 1 shows an Arrhenius plot of the rate constants for the reactions of $\text{Cl}^-(\text{D}_2\text{O})_{0-3}$ and $\text{Cl}^-(\text{H}_2\text{O})$ with CH_3Br . The rate constants for $n = 0$ are taken from a previous study.² We did remeasure the $n = 0$ rate constants at several temperatures and obtained excellent agreement with these previous results. The $n = 0$ reaction produces only Br^- and shows the negative temperature dependence that is typical of ion–molecule reactions, including most $\text{S}_{\text{N}}2$ reactions.^{10,31,32}

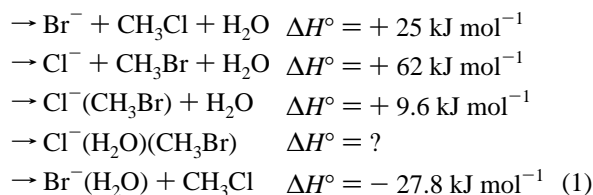
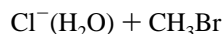
Addition of one water molecule to Cl^- changes the temperature dependence from negative to positive. The $n = 1$ reaction was studied from 238 to 478 K. No difference is found whether the ligand is H_2O or D_2O , i.e. we find no isotope effect. Using both the H_2O and D_2O data sets, the $n = 1$ rate constant is well described by the Arrhenius equation $k = (6.0 \times 10^{-10}) \exp(-1270/T) \text{ cm}^3 \text{ s}^{-1}$, which corresponds to an activation energy of 10.3 kJ mol^{-1} and a room temperature rate constant of $9 \times 10^{-12} \text{ cm}^3 \text{ s}^{-1}$. Three product ions were observed: Br^- , $\text{Cl}^-(\text{CH}_3\text{Br})$, and, at the lowest temperature, $\text{Cl}^-(\text{CH}_3\text{Br})(\text{D}_2\text{O})$ or $\text{Cl}^-(\text{CH}_3\text{Br})(\text{H}_2\text{O})$. We write the product as $\text{Cl}^-(\text{CH}_3\text{Br})$ and not $\text{Br}^-(\text{CH}_2\text{Cl})$ for reasons given below. Table 1 gives the observed product fractions as a function of temperature. In the presence of CH_3Br , the Cl^- signal decayed more slowly when $\text{Cl}^-(\text{D}_2\text{O})$ was injected into the tube than when only Cl^- was injected into the flow tube. Thus, it is probable that Cl^- is a minor product of the $\text{Cl}^-(\text{D}_2\text{O}) + \text{CH}_3\text{Br}$ reaction or that a

(31) Magnera, T. F.; Kebarle, P. In *Ionic Processes in the Gas Phase*; Almoester Ferreira, M. A., Ed.; D. Reidel Publishing: Boston, 1984; pp 135–157.

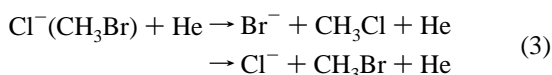
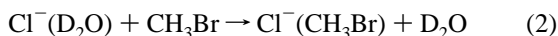
(32) Ikezoe, Y.; Matsuoka, S.; Takebe, M.; Viggiano, A. A. *Gas Phase Ion–Molecule Reaction Rate Constants Through 1986*; Maruzen Company, Ltd.: Tokyo, 1987.

portion of the $\text{Cl}^-(\text{D}_2\text{O})$ and $\text{Cl}^-(\text{CH}_3\text{Br})$ dissociate upon sampling to produce Cl^- .

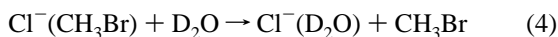
The reaction enthalpies of the possible product channels are listed below



Thermodynamic data are taken from Lias *et al.*,³³ Keesee and Castleman,³⁴ McMahon *et al.*³⁵ and Li *et al.*³⁶ Although the $\text{Br}^-(\text{H}_2\text{O})$ product channel is exothermic, $\text{Br}^-(\text{H}_2\text{O})$ was not observed over the entire temperature range of this study. It may be possible that $\text{Br}^-(\text{H}_2\text{O})$ is produced *via* the $\text{S}_{\text{N}}2$ mechanism and subsequently dissociates to Br^- and H_2O . However, in a previous study²⁵ we were able to observe significant quantities of $\text{Br}^-(\text{H}_2\text{O})$ produced by the $\text{OH}^-(\text{H}_2\text{O}) + \text{CH}_3\text{Br}$ reaction at temperatures ranging from 163 to 477 K. Hence, the complete absence of $\text{Br}^-(\text{D}_2\text{O})$ for the $\text{Cl}^-(\text{D}_2\text{O}) + \text{CH}_3\text{Br}$ reaction indicates that this channel is negligible. The lack of an isotope effect also suggests that an $\text{S}_{\text{N}}2$ mechanism is not operative: O'Hair *et al.* found significant isotope effects in the $\text{S}_{\text{N}}2$ reactions of $\text{F}^-(\text{H}_2\text{O})$ and $\text{F}^-(\text{D}_2\text{O})$ with methyl halides.³⁷ The 10.3 kJ mol⁻¹ activation energy observed for reaction 1 most closely matches the endothermicity of the ligand switching reaction to form $\text{Cl}^-(\text{CH}_3\text{Br})$ and is substantially lower than the endothermicity of the $\text{S}_{\text{N}}2$ channel to form Br^- directly. Our results indicate that the $\text{Cl}^-(\text{D}_2\text{O}) + \text{CH}_3\text{Br}$ reaction proceeds by a ligand switch to form $\text{Cl}^-(\text{CH}_3\text{Br})$ which then partially dissociates to Br^- and some Cl^- . Thus, we propose the following two-step mechanism



To test this mechanism, we added D_2O to the He in sufficient quantities to allow the exothermic ligand exchange reaction



to scavenge some of the $\text{Cl}^-(\text{CH}_3\text{Br})$ and compete with thermal dissociation (reaction 3), but not enough to affect the initial Cl^- to $\text{Cl}^-(\text{D}_2\text{O})$ ratio. The plot of the relevant ion signals *vs* $[\text{CH}_3\text{Br}]$ from such a test at 300 K is shown in Figure 2. Signals corresponding to $\text{Cl}^-(\text{D}_2\text{O})$, Br^- , and $\text{Cl}^-(\text{CH}_3\text{Br})$ with and without added D_2O are shown. The D_2O concentration, $3 \times 10^{11} \text{ cm}^{-3}$, is enough to convert only a small fraction of the Cl^- (approximately 10^{-4}) to $\text{Cl}^-(\text{D}_2\text{O})$.³² With added D_2O , the slope of the decay of the $\text{Cl}^-(\text{D}_2\text{O})$ signal is a factor of 3.5 less than without added D_2O , indicating that $\text{Cl}^-(\text{D}_2\text{O})$ is regenerated by reaction 4. In addition, the Br^- and $\text{Cl}^-(\text{CH}_3\text{Br})$ signals are

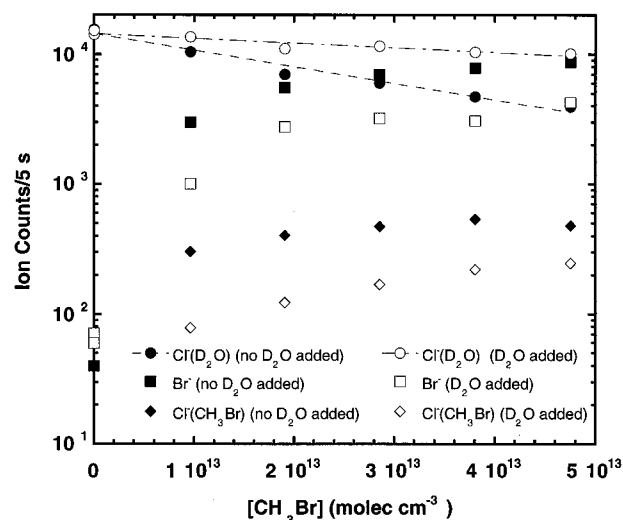


Figure 2. Count rates *vs* $[\text{CH}_3\text{Br}]$ at 300 K with and without D_2O added. The lines are exponential fits to the $\text{Cl}^-(\text{D}_2\text{O})$ signals.

both reduced when D_2O is added. Similar results were obtained for a variety of D_2O concentrations. These results all support the proposed mechanism, showing that the direct $\text{S}_{\text{N}}2$ channel is small or nonexistent. The fact that D_2O scavenges the dissociating complex to form $\text{Cl}^-(\text{D}_2\text{O})$ also shows that the complex is correctly written as $\text{Cl}^-(\text{CH}_3\text{Br})$ and not $\text{Br}^-(\text{CH}_3\text{Cl})$.

The breakup rate of the $\text{Cl}^-(\text{CH}_3\text{Br})$ complex can be determined from the $\text{Cl}^-(\text{D}_2\text{O})$ and $\text{Cl}^-(\text{CH}_3\text{Br})$ signals obtained as a function of $[\text{CH}_3\text{Br}]$ (in the absence of added D_2O). We have used a computer program which implements a variable-step fourth-order Runge-Kutta algorithm to integrate the rate equations resulting from reactions 2 and 3 as a function of $[\text{CH}_3\text{Br}]$. This program performs a χ^2 minimization by varying the values of k_2 , k_3 , and the $\text{Cl}^-(\text{D}_2\text{O})$ signal at $t = 0$. The value of the $\text{Cl}^-(\text{CH}_3\text{Br})$ signal was assumed to be zero at $t = 0$. This approach produced excellent fits to the data, including k_2 values that agreed well with the values taken in the usual manner. Figure 3 contains a set of typical plots. The resulting thermal dissociation rate constants, k_3 , are shown in Figure 4 as an Arrhenius plot. We estimate that the rate constants have an absolute accuracy of $\pm 40\%$ and a relative accuracy of $\pm 20\%$. The relative error bars are shown in the Figure 4. The dissociation rate constant is well-described by $k_3 = (4.5 \times 10^{-10}) \exp(-2260/T) \text{ cm}^3 \text{ s}^{-1}$ which corresponds to an activation energy of 18.8 kJ mol⁻¹. The error in the activation energy is estimated as $\pm 2.5 \text{ kJ mol}^{-1}$ based on taking the 20% error at the lowest and highest temperatures.

In deriving the thermal decomposition rate constants we assumed that only helium was responsible. At the highest flow rates of CH_3Br used, the fraction of CH_3Br in the tube was only 0.005. Assuming a β_0 , the low-pressure collision efficiency, of 1 for CH_3Br results in a maximum error of only 25%. Most of the data were taken with less than this flow rate of CH_3Br , and most likely β_0 is considerably less than 1,^{38,39} these facts indicate that the assumption causes a negligible error.

We also used this approach to estimate the dissociation branching fractions of the Br^- and Cl^- product channels of reaction 3. In this case we included the effect of the reaction of Cl^- with methyl bromide,



The Cl^- , $\text{Cl}^-(\text{D}_2\text{O})$, Br^- , and $\text{Cl}^-(\text{CH}_3\text{Br})$ data points were fitted

(33) Lias, S. G.; Bartmess, J. E.; Liebman, J. F.; Holmes, J. L.; Levin, R. D.; Mallard, W. G. *J. Phys. Chem. Ref. Data* **1988**, *17*, Suppl. 1, 1–861.

(34) Keesee, R. G.; Castleman, A. W., Jr. *J. Phys. Chem. Ref. Data* **1986**, *15*, 1011.

(35) McMahon, T. B. Personal communication.

(36) Li, C.; Ross, P.; Szulejko, J. E.; McMahon, T. B. *J. Am. Chem. Soc.* In press.

(37) O'Hair, R. A. J.; Davico, G. E.; Hacıoglu, J.; Dang, T. T.; DePuy, C. H.; Bierbaum, V. M. *J. Am. Chem. Soc.* **1994**, *116*, 3609–3610.

(38) Troe, J. *J. Chem. Phys.* **1977**, *66*, 4745.

(39) Tardy, D. C.; Rabinovitch, B. S. *Chem. Rev.* **1977**, *77*, 369.

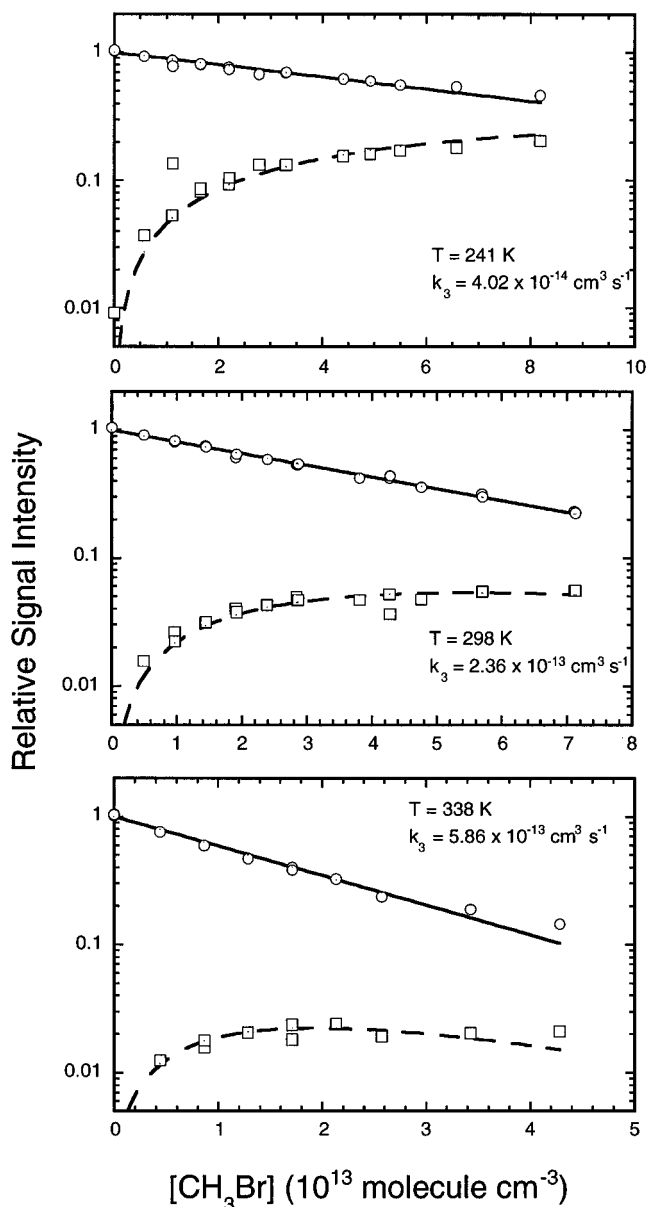


Figure 3. Typical plots used to determine the rate constants for the decomposition of $\text{Cl}^-(\text{CH}_3\text{Br})$. The circles represent the $\text{Cl}^-(\text{D}_2\text{O})$ signal and the squares represent the $\text{Cl}^-(\text{CH}_3\text{Br})$ signal.

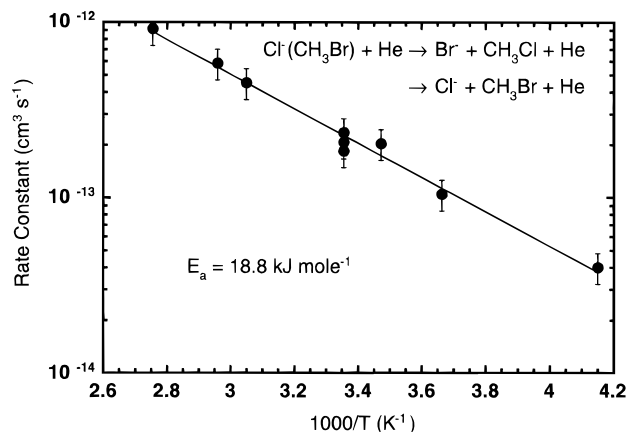


Figure 4. Arrhenius plot of the rate constant for the decomposition of $\text{Cl}^-(\text{CH}_3\text{Br})$.

by integrating the rate equations resulting from reactions 2, 3, and 5, and varying the values of k_2 , k_3 , the reaction 3 branching fraction, and the Cl^- and $\text{Cl}^-(\text{D}_2\text{O})$ signals at $t = 0$. The value

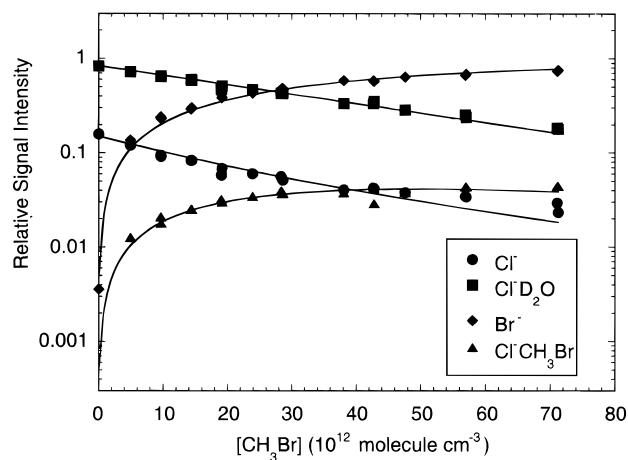
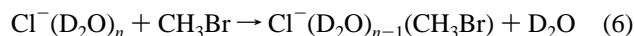


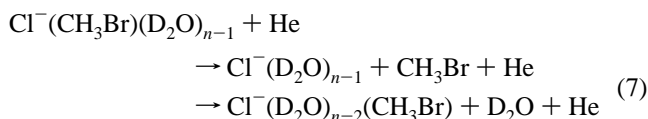
Figure 5. Count rates *vs* $[\text{CH}_3\text{Br}]$ at 300 K. The lines are the model fits to the data as described in the text.

of k_5 was assumed to be proportional to k_2 , with the proportionality constant determined from the Arrhenius expressions shown in Figure 1. A typical fit to the data is shown in Figure 5. This analysis indicated that the fraction of Br^- produced from reaction 3 was 90% and the fraction of Cl^- produced was 10%. However, it is probable that a small portion of $\text{Cl}^-(\text{D}_2\text{O})$ and $\text{Cl}^-(\text{CH}_3\text{Br})$ clusters break up upon sampling to produce Cl^- . If sampling breakup is also included in the model then equally good fits are obtained for 100% of the reaction proceeding *via* the Br^- channel with a 4% breakup upon sampling. Thus, our data place limits on the Cl^- formation channel at 0–10%.

We studied the reactions of $\text{Cl}^-(\text{D}_2\text{O})_{2,3}$ over more limited temperature ranges. The $n = 2$ reaction was studied from 203 to 298 K. The $n = 2$ rate constants were fit by $k = (4.4 \times 10^{-9}) \exp(-1329/T) \text{ cm}^3 \text{ s}^{-1}$ corresponding to an activation energy of 11.5 kJ mol^{-1} . This value is slightly larger than the activation energy observed for the $n = 1$ reaction. The $n = 3$ reaction was studied at 188 and 203 K. The main ionic product for both $n = 2$ and 3 was $\text{Cl}^-(\text{D}_2\text{O})_{n-1}$. No hydrates of Br^- were observed. In analogy to the mechanism for $\text{Cl}^-(\text{D}_2\text{O})$, we propose the following mechanism for $\text{Cl}^-(\text{D}_2\text{O})_{2,3}$,



followed by



For $n = 2$, 95% $\text{Cl}^-(\text{D}_2\text{O})$ and 5% $\text{Cl}^-(\text{D}_2\text{O})(\text{CH}_3\text{Br})$ were observed as products at 233 K, while 50% $\text{Cl}^-(\text{D}_2\text{O})$ and 50% $\text{Cl}^-(\text{D}_2\text{O})(\text{CH}_3\text{Br})$ were observed at 203 K. The temperature dependence associated with these products is consistent with the proposed mechanism, i.e. reaction 7 is considerably slower at lower temperatures. For $n = 3$, 90% $\text{Cl}^-(\text{D}_2\text{O})_2$, 8% $\text{Cl}^-(\text{D}_2\text{O})_2(\text{CH}_3\text{Br})$, and 2% $\text{Cl}^-(\text{D}_2\text{O})(\text{CH}_3\text{Br})$ were observed as products at 203 K, and 90% $\text{Cl}^-(\text{D}_2\text{O})_2$, 5% $\text{Cl}^-(\text{D}_2\text{O})_2(\text{CH}_3\text{Br})$, and 5% $\text{Cl}^-(\text{D}_2\text{O})(\text{CH}_3\text{Br})$ were observed at 188 K.

RRKM Modeling of $\text{Cl}^-(\text{CH}_3\text{Br})$ Dissociation

Rice–Ramsperger–Kassel–Marcus (RRKM) theory^{40–43} calculations were performed for $\text{Cl}^-(\text{CH}_3\text{Br})$ dissociation in the

(40) Robinson, P. J.; Holbrook, K. A. *Unimolecular Reactions*; Wiley-Interscience: London, 1972.

low-pressure limit, to give a more detailed analysis of the results in Figure 4 and to determine the branching ratio for $\text{Cl}^-(\text{CH}_3\text{Br})$ dissociation to Cl^- and Br^- . According to RRKM theory, the thermal unimolecular rate constant in the low-pressure limit may be expressed as^{40–42,44}

$$k_0(T) = \frac{\beta_0 \omega}{Q} \int_{E_0}^{\infty} dE \sum_{J=0}^{J_{\max}(E)} (2J+1) \rho(E, J) \exp\left(-\frac{E}{k_B T}\right) \quad (8)$$

where β_0 is the low-pressure collision efficiency,^{38–42,44–47} ω is the collision frequency, Q is the vibrational/rotational partition function for the unimolecular reactant, and $\rho(E, J)$ is the reactant's density of states. E_0 is the unimolecular threshold, and $J_{\max}(E)$ is the largest value of J for which the reaction can occur for energy E . If the reactant is treated as a symmetric top, with the rotational quantum number K treated as active,^{44,48,49} $\rho(E, J)$ is given by

$$\rho(E, J) = \sum_{K=-J}^J \rho(E, J, K) \quad (9)$$

with

$$\rho(E, J, K) = \rho[E - E_r(J, K)] \quad (10)$$

where $E_r(J, K)$ is the symmetric top rotational energy.

The energies and vibrational frequencies used to evaluate eq 8 are those for the analytic potential energy function PES1(Br), derived from *ab initio* calculations to represent the $\text{Cl}^- + \text{CH}_3\text{Br} \rightarrow \text{ClCH}_3 + \text{Br}^-$ reaction.¹² The minimum energy pathway from this work is shown in Figure 6. The classical well depth for $\text{Cl}^-(\text{CH}_3\text{Br})$ on PES1(Br) is $-44.89 \text{ kJ mol}^{-1}$. Using harmonic frequencies to approximate the CH_3Br and $\text{Cl}^-(\text{CH}_3\text{Br})$ zero-point energies⁵⁰ gives a $\text{Cl}^-(\text{CH}_3\text{Br}) \rightarrow \text{Cl}^- + \text{CH}_3\text{Br}$ 0 K dissociation energy, D_0 , of 42.3 kJ mol^{-1} , which agrees with the measured value of $42 \pm 4 \text{ kJ mol}^{-1}$.¹⁰ The transition state for $\text{Cl}^-(\text{CH}_3\text{Br}) \rightarrow \text{Cl}^- + \text{CH}_3\text{Br}$ is variational,^{51–56} and the counteracting effects of the increased transitional mode bending frequencies and the more attractive radial potential as Cl^- and CH_3Br associate results in a unimolecular dissociation threshold E_0 equal to the above dissociation energy D_0 .

(41) Forst, W. *Theory of Unimolecular Reactions*; Academic Press: New York, 1973.

(42) Gilbert, R. G.; Smith, S. C. *Theory of Unimolecular and Recombination Reactions*; Blackwell: London, 1990.

(43) Baer, T.; Hase, W. L. *Unimolecular Reaction Dynamics. Theory and Experiment*; New York: Oxford, 1996.

(44) Zhu, L.; Chen, W.; Hase, W. L.; Kaiser, E. W. *J. Phys. Chem.* **1993**, *97*, 311.

(45) Chan, S. C.; Rabinovitch, B. S.; Bryant, J. T.; Spicer, L. D.; Fujimoto, T.; Lin, Y. N.; Paulou, S. P. *J. Phys. Chem.* **1970**, *74*, 3160.

(46) Fujimoto, T.; Lin, Y. N.; Paulou, S. P. *J. Phys. Chem.* **1970**, *74*, 3160.

(47) Troe, J. *J. Phys. Chem.* **1979**, *83*, 114.

(48) Zhu, L.; Hase, W. L. *Chem. Phys. Lett.* **1990**, *175*, 117.

(49) Aubanel, E. E.; Wardlaw, D. M.; Zhu, L.; Hase, W. L. *Int. Rev. Phys. Chem.* **1990**, *10*, 249.

(50) The harmonic model should give an accurate zero-point energy difference for CH_3Br and $\text{Cl}^-(\text{CH}_3\text{Br})$, since there is very little shifting in the vibrational frequencies in going from the reactant to complex.

(51) Bunker, D. L.; Pattengill, M. *J. Chem. Phys.* **1968**, *48*, 772.

(52) Hase, W. L. *J. Chem. Phys.* **1972**, *57*, 730.

(53) Hase, W. L. In *Modern Theoretical Chemistry, Vol. 2, Dynamics of Molecular Collisions*; Miller, W. H., Ed.; Plenum: New York, 1976; p 121.

(54) Hase, W. L. *Acc. Chem. Res.* **1983**, *16*, 258.

(55) Hase, W. L.; Wardlaw, D. M. In *Advances in Bimolecular Collisions*; Ashfold, M. N. R., Baggott, J. E., Ed.; Royal Society of Chemistry: London, 1989; p 171.

(56) Wardlaw, D. M.; Marcus, R. A. *Adv. Chem. Phys.* **1988**, *70*, 231.

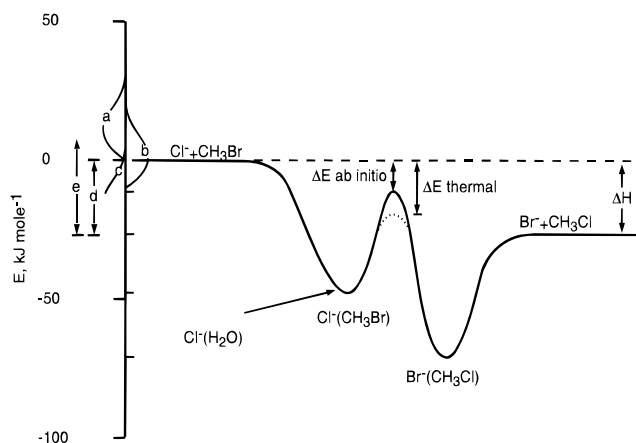


Figure 6. Potential energy surface for the reaction of $\text{Cl}^- + \text{CH}_3\text{Br}$ from Wang *et al.* Added to the graph is the barrier height derived from the thermal decomposition experiments reported here. Approximate energy distributions for experiments performed on this system are given on the axis as (a) chemical reaction at low pressure, (b) chemical reaction at 640 Torr, (c) the reacting part of the thermal decomposition experiments (note the tail goes slightly above zero), (d) distribution range of decaying states in the Graul and Bowers experiments and collisional activation of the exit well complex, and (e) distribution range of decaying states in collisional activation of the entrance well complex.

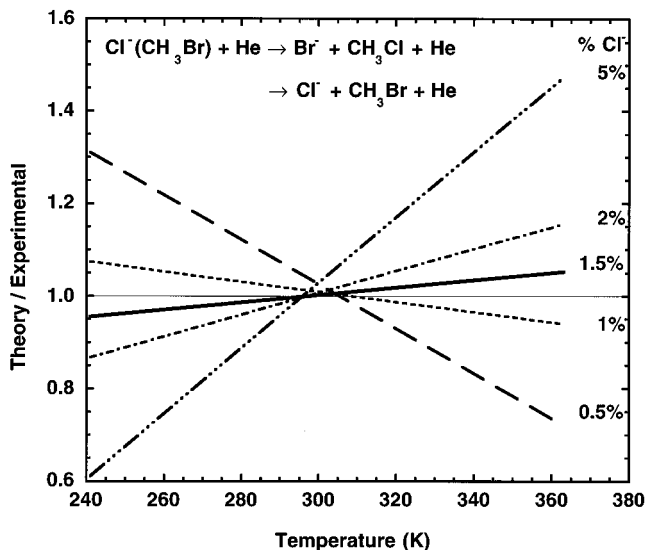


Figure 7. Plot of RRKM rate constant divided by the experimental rate constant *vs* temperature for the thermal decomposition of $\text{Cl}^-(\text{CH}_3\text{Br})$. Plotted are least-squares fits for several assumed values of the branching into Cl^- . Several other values of the Cl^- branching fraction were performed but not included in the graph for clarity. The ideal is the horizontal line through 1.

Equation 8 was used to calculate $k_0(T)$ values for $\text{Cl}^-(\text{CH}_3\text{Br})$ dissociation to $\text{Cl}^- + \text{CH}_3\text{Br}$ and $\text{ClCH}_3 + \text{Br}^-$. The threshold energy E_0 for the latter dissociation channel is given by the central barrier height on the potential energy surface. This threshold was adjusted so that varying fractions of Br^- and Cl^- were produced. For a particular threshold these fractions vary with temperature. To determine an absolute (not relative) value for the decomposition rate constant, He and $\text{Cl}^-(\text{CH}_3\text{Br})$ were assigned collision diameters of 2.2 and 8.5 Å,⁴⁵ respectively, to give $\omega = (14.8 \times 10^7)P \text{ Torr s}^{-1}$ and the collision efficiency β_0 was taken as an adjustable parameter. The thermal dissociation rates were normalized by adjusting the β parameter so that the calculations matched the 300 K experimental point. Figure 7 shows the theoretical result obtained in this manner divided by the experimental value as a function of temperature for

Table 2. Calculated Branching into Cl^- for the Thermal Dissociation of $\text{Cl}^-(\text{CH}_3\text{Br})$

temp (K)	Cl^- product (%)
241	0.3
273	0.8
298	1.5
328	2.7
363	4.8

various fractions of Cl^- produced. A straight line with no slope represents the best fit to the data. From Figure 7 it can be seen that the fit with 1.5% Cl^- at 298 K gives the best reproduction of the experimental temperature dependence with a value of 1% at 298 K only slightly worse. Values as close as 0.5 and 2% give clearly negative and positive slopes, respectively. The 1.5% Cl^- fit results in a value for the $\text{Cl}^-(\text{CH}_3\text{Br}) \rightarrow \text{Br}^- + \text{CH}_3\text{Cl}$ threshold of 22.5 kJ mol^{-1} and the value chosen for β_0 is 2.0×10^{-2} . The barrier height is shown in Figure 6 as ΔE thermal. For Cl^- fractions of 1 and 2% at 298 K, the threshold values are 21.0 and 23.7 kJ mol^{-1} , respectively. We report this number as $22.5 \pm 2.5 \text{ kJ mol}^{-1}$. The fraction of Cl^- produced in the decomposition was calculated to increase with increasing temperature as expected, and the results are listed in Table 2.

Since the $\text{Cl}^-(\text{CH}_3\text{Br}) \rightarrow \text{Cl}^- + \text{CH}_3\text{Br}$ dissociation threshold is 42.3 kJ mol^{-1} for these calculations, the above fitted threshold of $22.5 \pm 2.5 \text{ kJ mol}^{-1}$ for Br^- formation suggests the threshold energy difference ΔE_0 for Cl^- and Br^- formation is 19.8 kJ mol^{-1} . This value for ΔE_0 is significantly larger than the values in the range of 4.6 to 6.3 kJ mol^{-1} derived¹⁴ by using different statistical models to fit the experimental 300 K, low-pressure $\text{Cl}^- + \text{CH}_3\text{Br} \rightarrow \text{ClCH}_3 + \text{Br}^-$ rate constant.¹ These smaller values for ΔE_0 are similar to the *ab initio* values of 4.2 and 6.7 kJ mol^{-1} determined from MP2/PTZ⁵⁷ and G2(+)⁵⁸ calculations, respectively.

The above comparisons indicate the $\text{Cl}^-(\text{CH}_3\text{Br}) \rightarrow \text{ClCH}_3 + \text{Br}^-$ barrier derived here of 22.5 kJ mol^{-1} may be $\sim 15 \text{ kJ mol}^{-1}$ lower than the actual barrier. This is larger than our 2.5 kJ mol^{-1} uncertainty in our experimental activation energy for the overall decomposition. The origin(s) of this discrepancy is unclear. One might want to consider non-statistical effects for $\text{Cl}^-(\text{CH}_3\text{Br})$ decomposition, which may make RRKM theory, i.e. eq 8, invalid for calculating $k_0(T)$. However, this seems unlikely since non-RRKM effects are more prevalent at high pressure, when collisional quenching competes with intramolecular vibrational energy redistribution (IVR).^{53,59} On the other hand, the low pressure and long time between collisions ($\sim 10^{-7}$ s) suggest that a dynamical process not included in calculating $k_0(T)$ for $\text{Cl}^-(\text{CH}_3\text{Br}) \rightarrow \text{ClCH}_3 + \text{Br}^-$, i.e. tunneling through the central barrier, may be important. Using eq 8, with a tunneling correction, to fit the experimental Cl^- to Br^- branching ratio will require a central barrier height higher than the value of 22.5 kJ mol^{-1} derived here without tunneling. In the bimolecular reaction the energy is greater than that of the barrier and tunneling would not be important.

Calculating an accurate correction for low-pressure tunneling through the central barrier will require evaluating state specific tunneling rates,^{60–62} which are thermally averaged. Also, because of the sharp curvature for the $\text{Cl}^-(\text{CH}_3\text{Br}) \rightarrow \text{ClCH}_3$

+ Br^- reaction path,^{63,64} it is very likely that the most important tunneling paths will not follow the reaction path, but involve multidimensional “corner cutting”.^{65–67} Determining an accurate tunneling correction will require extensive potential energy surface modeling in the vicinity of the central barrier between the two complex minima. Therefore, at this time we leave such a detailed calculation to future work. It is of interest that there has been no consideration of tunneling in presentations outlining RRKM calculations for thermal systems at low pressure.^{40–42} The only careful study of this effect appears to be for vinyl radical decomposition, for which tunneling at low pressures was found to be very important.⁶⁸

This comparison shows that an RRKM model, which neglects tunneling and uses a central barrier height lower than the *ab initio* barrier, fits the temperature dependence of the data extremely well. Finally, the above RRKM calculation uses a harmonic density of states. The anharmonic density is approximately two times larger,⁶⁹ and using this density would require a β_0 two times smaller to fit experiment.

The measured activation energy of $18.8 \pm 2.5 \text{ kJ mol}^{-1}$ is smaller than the effective barrier of 22.5 kJ mol^{-1} derived from the RRKM calculations. This is expected for thermal dissociation reactions in the low pressure limit.^{17,18} The principle behind this is that the activation energy is the average energy of reacting molecules minus the average energy of reactants. In the low-pressure limit the average energy of reacting molecules is just above the critical energy for reaction, i.e. significantly smaller than this same energy for a Boltzmann distribution. In the high-pressure limit we would find the activation energy approximately equal to the central barrier height to $\text{Cl}^-(\text{CH}_3\text{Br}) \rightarrow \text{Br}^- + \text{CH}_3\text{Cl}$ dissociation.

Discussion

For the $\text{Cl}^-(\text{D}_2\text{O})_n + \text{CH}_3\text{Br}$ system, we find that the $\text{S}_{\text{N}}2$ mechanism is only important for the $n = 0$ case. For $n > 0$ we observe ligand switching presumably because the relative height of the central barrier becomes too high for the $\text{S}_{\text{N}}2$ mechanism to be efficient. This result is to be expected because the barrier crossing efficiency for the $n = 0$ case is already quite low (1%) and the relative height of the central barrier is believed to increase with increasing hydration level.¹⁹

Ligand switching mechanisms have not been previously reported for the reactions of hydrated ions with methyl halides. However, previous studies have mostly focused on reactions involving F^- or OH^- . At low levels of hydration, F^- and OH^- form substantially stronger bonds with water than does Cl^- .³⁴ As a result ligand switching with hydrates of F^- and OH^- is probably much more endothermic. The *ab initio* studies of Morokuma and co-workers^{70,71} support this statement. They calculate that the reaction $\text{OH}^-(\text{H}_2\text{O}) + \text{CH}_3\text{Cl} \rightarrow \text{Cl}^-(\text{CH}_3\text{Cl}) + \text{H}_2\text{O}$ is endothermic by 57 kJ mol^{-1} , while the reaction $\text{Cl}^-(\text{H}_2\text{O}) + \text{CH}_3\text{Cl} \rightarrow \text{Cl}^-(\text{CH}_3\text{Cl}) + \text{H}_2\text{O}$ is endothermic by only 4 kJ mol^{-1} .

(63) Cho, Y. J.; Vande Linde, S. R.; Zhu, L.; Hase, W. L. *J. Chem. Phys.* **1992**, *96*, 8275.

(64) Wang, H.; Hase, W. L. *Chem. Phys.* Submitted for publication.

(65) Marcus, R. A.; Coltrin, M. E. *J. Chem. Phys.* **1977**, *67*, 2609.

(66) Garrett, B. C.; Truhlar, D. G.; Wagner, A. F.; Dunning, T. H. *J. Chem. Phys.* **1985**, *78*, 440.

(67) Garrett, B. C.; Joseph, T.; Truong, T.; Truhlar, D. G. *Chem. Phys.* **1989**, *136*, 271.

(68) Knyazev, V. D.; Slagle, I. R. *J. Phys. Chem.* Submitted for publication.

(69) Peslherbe, G. H.; Wang, H.; Hase, W. L. *J. Chem. Phys.* **1995**, *102*, 5626.

(70) Morokuma, K. *J. Am. Chem. Soc.* **1982**, *104*, 3732.

(71) Ohta, K.; Morokuma, K. *J. Phys. Chem.* **1985**, *89*, 5845.

(57) Hu, W.-P.; Truhlar, D. G. *J. Am. Chem. Soc.* **1995**, *117*, 10726.

(58) Glukhovtsev, M. N.; Pross, A.; Radom, L. *J. Am. Chem. Soc.* Submitted for publication.

(59) Meagher, J. F.; Chao, K. J.; Barker, J. R.; Rabinovitch, B. S. *J. Phys. Chem.* **1974**, *78*, 2535.

(60) Miller, W. H. *J. Am. Chem. Soc.* **1979**, *101*, 6810.

(61) Kato, S.; Morokuma, K. *J. Chem. Phys.* **1980**, *72*, 206.

(62) Forst, W. *J. Phys. Chem.* **1983**, *87*, 4489.

Two previous studies of solvated chloride ions with methyl bromide have been made. Bohme and Raksit²¹ studied the reactions of $\text{Cl}^-(\text{S})_n$ with CH_3Br , where $\text{S} = \text{CH}_3\text{OH}$, $\text{C}_2\text{H}_5\text{OH}$, CH_3COCH_3 , HCOOH , and CH_3COOH . They found that the reaction rate constants were too low for accurate measurement for $n \geq 1$ and did not observe ligand switching. Giles and Grimsud²⁶ found that solvation of Cl^- by CHCl_3 also inhibits the reaction with CH_3Br and, similarly, did not find evidence for ligand switching. However, the experimental systems used in these studies produced solvated clusters by adding solvent directly to the reaction mixture. Hence, any $\text{Cl}^-(\text{S})_{n-1}\text{CH}_3\text{Br}$ produced would be quickly converted back into $\text{Cl}^-(\text{S})_n$ by the high levels of solvent in the flow (analogous to reaction 5). It is interesting to note that as the hydration levels of F^- , OH^- , and Cl^- are increased their water binding energies become similar. Thus, it is possible that ligand switching reactions will be observed for large ($n > 3$) hydrates of F^- and OH^- .

Our study of the thermal dissociation of $\text{Cl}^-(\text{CH}_3\text{Br})$ indicates that when the complex is formed *via* $\text{Cl}^-(\text{H}_2\text{O}) + \text{CH}_3\text{Br}$, it dissociates through the Br^- channel with a branching fraction greater than 90%. Several previous studies have also focused on the $\text{Cl}^-(\text{CH}_3\text{Br})$ complex due to its role as the initial intermediate in the unsolvated $\text{Cl}^- + \text{CH}_3\text{Br}$ reaction. At low pressure (0.4 Torr) the $\text{Cl}^- + \text{CH}_3\text{Br}$ reaction proceeds at 1% of the collision rate. Thus, 99% of the $\text{Cl}^-(\text{CH}_3\text{Br})$ collision complexes dissociate back into Cl^- and CH_3Br , while 1% of the complexes dissociate into Br^- and CH_3Cl . At high pressure (640 Torr of N_2) the reaction proceeds at 3% of the collision rate, which corresponds to 97% of the complexes dissociating to Cl^- and CH_3Br .

Two previous studies have isolated the $\text{Cl}^-(\text{CH}_3\text{Br})$ complex and directly monitored its dissociation products. Cyr *et al.*⁵ prepared $\text{Cl}^-(\text{CH}_3\text{Br})$ in a supersonic expansion and activated the complex in a single high-energy collision (2.5 keV) with Ar. They observed the complex to dissociate with equal probability *via* the Cl^- and Br^- product channels. Graul and Bowers^{3,15} prepared a metastable beam of $\text{Cl}^-(\text{CH}_3\text{Br})$ which dissociated primarily *via* the Br^- channel and estimated that the Cl^- channel had a branching fraction of less than 1%. They also performed a collisional activation experiment and obtained good agreement with the work of Cyr *et al.*⁵

These differing results can be qualitatively reconciled by examining the energy of the complex in each experiment. The approximate energy distributions of each experiment are shown on the y axis in Figure 6. The curve marked (a) in Figure 6 represents a Boltzmann distribution of energies of the reactants for the $\text{Cl}^- + \text{CH}_3\text{Br}$ reaction. Trajectory calculations predict that the complex formed from the bare ion reaction has a lifetime of approximately 10 ps.¹³ For the low-pressure (0.5 Torr) flow tube experiments, collisions occur approximately every 5 ns. Thus, collisional cooling of the complex does not occur, and the energy distribution of the complex is very similar to distribution (a). Because the distribution lies substantially above the dissociation energy for either channel, the complex dissociates *via* the more entropically favored Cl^- channel 99% of the time.

The high-pressure kinetics study of the $\text{Cl}^- + \text{CH}_3\text{Br}$ reaction⁴ has the same energy distribution for reactants, but collisions with the complex occur approximately every 50 ps. Thus, the complex is cooled slightly by collisions. Curve (b) in Figure 6 is an estimate of the distribution. The lower energy causes more of the complexes to dissociate *via* the Br^- channel.

The distribution of the complex formed from the $\text{Cl}^-(\text{D}_2\text{O}) + \text{CH}_3\text{Br}$ ligand switching reaction is represented by curve (c).

Since $\text{Cl}^-(\text{CH}_3\text{Br})$ formation is endothermic, the complex is likely to be near the bottom of the well. However, the lifetime of the $\text{Cl}^-(\text{CH}_3\text{Br})$ cluster is long enough (>0.1 ms) to allow thousands of collisions with the bath gas to establish a Boltzmann distribution truncated by the thermal dissociation process. The dominance of the Br^- channel indicates that the majority of the complexes have energies less than the threshold for separating Cl^- and CH_3Br . It also should be noted that the large difference between the dissociation branching ratios obtained from complexes prepared *via* $\text{Cl}^-(\text{D}_2\text{O}) + \text{CH}_3\text{Br}$ and those prepared in the high pressure kinetics study *via* $\text{Cl}^- + \text{CH}_3\text{Br}$ indicates that the atmospheric pressure study had not reached the high-pressure limit.

The collisional activation (CAD) experiments have less-well-defined distributions. Cyr *et al.*⁵ estimated that the complex had an average energy of 0.65 eV and a width on the order of 1 eV. This distribution should have substantial populations of $\text{Cl}^-(\text{CH}_3\text{Br})$ complexes both below and above the threshold dissociating to $\text{Cl}^- + \text{CH}_3\text{Br}$. Thus their estimated energy distribution and equally divided product distribution are consistent.

The metastable decay experiments of Graul and Bowers^{3,15} produced little or no Cl^- , indicating that few of the dissociating complexes have an energy above the $\text{Cl}^- + \text{CH}_3\text{Br}$ asymptote, and hence, their energy spread is likely to be similar to that obtained from the $\text{Cl}^-(\text{D}_2\text{O}) + \text{CH}_3\text{Br}$ reaction, although the distribution may be different.

The results reported here demonstrate that RRKM theory can model the dissociation of $\text{Cl}^-(\text{CH}_3\text{Br})$ when it is formed by the $\text{Cl}^-(\text{D}_2\text{O}) + \text{CH}_3\text{Br}$ reaction if a smaller central barrier is used. In contrast, previous experimental² and theoretical¹⁴ studies indicate that the breakup of $\text{Cl}^-(\text{CH}_3\text{Br})$ cannot be modeled by RRKM theory when formed by the $\text{Cl}^- + \text{CH}_3\text{Br}$ reaction. This difference is most likely due to the lifetimes of the resulting complexes. Complexes produced by $\text{Cl}^- + \text{CH}_3\text{Br}$ have energies substantially above the threshold for dissociating to $\text{Cl}^- + \text{CH}_3\text{Br}$ or $\text{Br}^- + \text{CH}_3\text{Cl}$ and have lifetimes on the order of picoseconds¹³ which is apparently insufficient to allow the energy to be randomly dispersed. In addition, complexes in high- J states may have an increased probability for nonstatistical behavior. Complexes produced by $\text{Cl}^-(\text{D}_2\text{O}) + \text{CH}_3\text{Br}$ reactions are initially formed at energies below the threshold for dissociating to either $\text{Cl}^- + \text{CH}_3\text{Br}$ or $\text{Br}^- + \text{CH}_3\text{Cl}$. These complexes may dissociate by tunneling or be further activated by collisions with He. The tunneling lifetime is expected to be sufficiently long for energy to be randomly distributed.

Graul and Bowers have also reported nonstatistical effects in their study of the dissociation of metastable $\text{Cl}^-(\text{CH}_3\text{Br})$.^{3,15} They found that the kinetic energy release by metastable $\text{Cl}^-(\text{CH}_3\text{Br})$ upon dissociation was 0.05–0.1 eV less than predicted by phase space theory. Metastable dissociation was observed to take place on the order of microseconds, a time similar to the thermal dissociation experiment. Therefore, the barrier needed to fit the thermal dissociation data should apply. This implies that the distribution in the metastable decay experiment would be about 15 kJ mol⁻¹ less energetic than used in the phase space calculations, about the same as the difference between the experimental results and the phase space calculations. The results would still be nonstatistical but due to tunneling through the barrier instead of incomplete energy randomization.

If the above is true, the following picture emerges: For energies above the dissociation limit to Cl^- and CH_3Br , the lifetime of the collision complex is short (\sim picoseconds), nonstatistical behavior occurs, and most of the dissociation is

via the Cl^- channel. As the energy is lowered, the lifetime increases to microseconds, as evidenced by the metastable decay experiments. Statistical theories using an effective barrier adequately describe the results, and the complex predominantly dissociates through the Br^- channel.

Conclusions

We have studied the reactions of $\text{Cl}^-(\text{D}_2\text{O})_{n=1-3}$ with $\text{CH}_3\text{-Br}$. We find that the $\text{S}_{\text{N}}2$ channel is negligible and that ligand switching becomes the main pathway. The shutdown of the $\text{S}_{\text{N}}2$ channel is consistent with past work that indicates solvation greatly hinders this mechanism.¹⁹⁻²⁵ The ligand switching products were observed to thermally dissociate in the helium buffer gas. For $n = 1$, the ligand switching produces the entrance well complex, $\text{Cl}^-(\text{CH}_3\text{Br})$, which then dissociates to produce mainly Br^- . RRKM calculations were carried out to fit the data. The barrier was adjusted to match the thermal dissociation rate, and excellent agreement was found when a barrier height of $22.5 \pm 2.5 \text{ kJ mol}^{-1}$ was used. This calculated barrier is significantly smaller than the *ab initio* barrier¹² and that obtained by modeling the $\text{Cl}^- + \text{CH}_3\text{Br}$ reaction.^{3,14,15} This leads us to speculate that tunneling may be important in the thermal decomposition experiments.

The hypothesis that statistical theories work well for $\text{S}_{\text{N}}2$ reactions when the lifetime is long and do not when the lifetime is short is consistent with other work from our laboratory on $\text{S}_{\text{N}}2$ reactions. We have found nonstatistical kinetics in systems involving methyl halides.^{2,72} Several theoretical studies involving halide ion reactions with methyl halides have shown that the lifetimes are short.^{13,63} In contrast, statistical behavior was found for reactions involving species other than methyl halides.^{16,17} For these reactions, we observed that a fraction of the reactivity proceeds by association. The association sets the lifetime of the complex in the 10^{-7} s range.

Acknowledgment. The PL authors thank John Williamson and Paul Mundis for technical support. Helpful discussions with Roger Meads, Susan Arnold, Caroline Dessent, and Mark Johnson are gratefully acknowledged. The research was supported by the Air Force Office of Scientific Research and the National Science Foundation.

JA960872U

(72) Su, T.; Morris, R. A.; Viggiano, A. A.; Paulson, J. F. *J. Phys. Chem.* **1990**, *94*, 8426.